Journal of Solid State Chemistry 183 (2010) 2516–2521

Contents lists available at ScienceDirect

Journal of Solid State Chemistry

journal homepage: www.elsevier.com/locate/jssc

The energetics of lanthanum tantalate materials

Tori Z. Forbes [a], May Nyman [b], Mark A. Rodriguez [b], Alexandra Navrotsky [a,*]

[a] Peter A. Rock Thermochemistry Laboratory and NEAT ORU, University of California at Davis, Davis, CA 95616, USA
[b] Sandia National Laboratory, POB 5800, Albuquerque, NM 87185, USA

ARTICLE INFO

Article history:
Received 6 May 2010
Received in revised form
11 August 2010
Accepted 18 August 2010
Available online 22 August 2010

Keywords:
Rare earth
Lanthanum
Tantalate
Calorimetry

ABSTRACT

Lanthanum tantalates are important refractory materials with application in photocatalysis, solid oxide fuel cells, and phosphors. Soft-chemical synthesis utilizing the Lindqvist ion, $[Ta_6O_{19}]^{8-}$, has yielded a new phase, $La_2Ta_2O_7(OH)_2$. Using the hydrated phase as a starting material, a new lanthanum orthotantalate polymorph was formed by heating to 850 °C, which converts to a previously reported $LaTaO_4$ polymorph at 1200 °C. The stabilities of $La_2Ta_2O_7(OH)_2$ (LaTa−OH), the intermediate $LaTaO_4$ polymorph (LaTa-850), and the high temperature phase (LaTa-1200) were investigated using high-temperature oxide melt solution calorimetry. The enthalpy of formation from the oxides were calculated from the enthalpies of drop solution to be -87.1 ± 9.6, -94.9 ± 8.8, and -93.1 ± 8.7 kJ/mol for LaTa−OH, LaTa-850, and LaTa-1200, respectively. These results indicate that the intermediate phase, LaTa-850, is the most stable. This pattern of energetics may be related to cation–cation repulsion of the tantalate cations. We also investigated possible $LnTaO_4$ and $Ln_2Ta_2O_7(OH)_2$ analogues of Ln=Pr, Nd to examine the relationship between cation size and the resulting phases.

Published by Elsevier Inc.

1. Introduction

Rare-earth tantalates are important refractory compounds having high chemical and electrochemical stability [1,2]. These materials, in both doped and undoped forms, show promise for many applications due to their photoelectronic activity [3], ionic conductivity [4,5], and luminescence properties [6–12]. Applications currently being explored include photocatalysis for H_2 production [13–18], photodecomposition of contaminants [19,20], electrolytes in solid oxide fuel cells (SOFCs) [21], and phosphors for light emitting diodes (LEDs) [22].

The chemical stability of the rare-earth tantalates is advantageous for applications, but challenging for the development of new materials. Traditional synthesis routes require solid state processing with repeated milling and high reaction temperatures up to 1600 °C [2,21]. The resulting rare-earth orthotantalates (La:Ta 1:1) are primarily of the composition $LnTaO_4$. A majority of the rare-earth tantalates (Ln=Nd, Sm, Gd, Tb, Dy, Ho, Er, Yb) with this stoichiometry crystallize in the monoclinic fergusonite structure at lower temperature and the tetragonal scheelite structure above 1300 °C [1,23–25]. The light lanthanides (Ln=La, Ce, and Pr) are also reported to crystallize in the orthorhombic space group, $Cmc2_1$ [26].

In the interest of expanding the solid-state chemistry of the rare-earth tantalates other synthesis procedures are being explored including sol–gel techniques and exchange reactions [27–29]. Traditional aqueous routes were initially unsuccessful due to the incompatibility of the acid soluble rare-earth oxides and the base soluble tantalates. However, Nyman et al. [30] developed a hydrothermal process in which the Lindqvist ion polyoxometalate $[Ta_6O_{19}]^{8-}$ and citrate-complexed rare earths could be utilized to synthesize new materials: a hydrated phase, $Ln_2Ta_2O_7(OH)_2$ for larger rare earths (La through Sm) and $KLnTa_2O_7$ perovskite for smaller rare earths (Y, Eu–Lu) [22]. Heating $La_2Ta_2O_7(OH)_2$ to 850 °C also produced a new $LaTaO_4$ polymorph, which converted to a high temperature polymorph [26] at 1200 °C. This novel $LaTaO_4$ polymorph forms cleanly at 850 °C and crystallizes in the orthorhombic space group *Pbca* with a=7.8286(1) Å, b=11.2180(1) Å, and c=7.4642(1) Å [31].

The new $LaTaO_4$ polymorph has so far only been formed by the dehydration of the $La_2Ta_2O_7(OH)_2$ precursor through the following reaction [31]:

$$La_2Ta_2O_7(OH)_2 \rightarrow LaTaO_4\ (850\ ^\circ C) \rightarrow LaTaO_4\ (1200\ ^\circ C)$$

Understanding the energetics of the reaction and the thermodynamic stabilities of the three lanthanum tantalate compounds could give insight into the importance of this intermediate phase for chemical applications and the viability of this synthesis route for other novel rare-earth tantalate materials. The current study uses the high-temperature oxide melt drop solution calorimetry to investigate the energetics of the precursor phase

* Corresponding author.
E-mail addresses: tmforbes@ucdavis.edu (T.Z. Forbes), mdnyman@sandia.gov (M. Nyman), marodri@sandia.gov (M.A. Rodriguez), anavrotsky@ucdavis.edu (A. Navrotsky).

0022-4596/$ - see front matter Published by Elsevier Inc.
doi:10.1016/j.jssc.2010.08.024

$La_2Ta_2O_7(OH)_2$ (designated LaTa–OH), the intermediate $LaTaO_4$ polymorph (LaTa-850), and the high temperature $LaTaO_4$ polymorph (LaTa-1200). In this study, we have also characterized the thermal decomposition of the praseodymium and neodymium tantalate analogues to compare to that of the lanthanum tantalates. The relationship between the structure and the relative stabilities of the rare-earth tantalates and the implications for the formation of intermediate phase polymorphs for other rare-earth tantalates are discussed.

2. Experimental methods

2.1. Synthesis and characterization

Approximately 200 mg of LaTa–OH, LaTa-850, and LaTa-1200 were synthesized according to previously reported methods [30,31]. Briefly, the LaTa–OH sample was prepared by initially precipitating a lanthanum citrate precursor by combining lanthanum chloride (0.42 g in 4 g DI water, 1.35 mmol) and potassium citrate tribasic (0.44 g in 3 g DI water, 1.35 mmol). Potassium hydroxide was added to dissolve the lanthanum citrate precipitate and then the polyoxometalate, $K_7Na[Ta_6O_{19}]\cdot 14H_2O$ (0.42 g in 2 g of DI water, 1.35 mmol), was added to the solution. The solution was placed in a Parr reactor at 220 °C for 3 days. The resulting off-white LaTa–OH powder (~100% yield) was collected by vacuum filtration and washed several times with DI water and methanol. The $LaTaO_4$ polymorphs were subsequently synthesized by heating the LaTa–OH powder for 2 h at 850 and 1200 °C to form LaTa-850 and LaTa-1200. The synthesis of $Pr_2Ta_2O_7(OH)_2$ and $Nd_2Ta_2O_7(OH)_2$ structural analogues of LaTa–OH was described prior [30], and unit cell parameters and atomic positions were refined based on the LaTa–OH structure.

The phase purity of the samples was verified using X-ray diffraction and electron microprobe analysis. Powder X-ray diffraction pattern of the samples were collected using a Bruker Advance diffractometer equipped with a LynxEye solid state detector. The pattern was collected using copper radiation (λ=1.5418 Å) from 10° to 90° 2θ with a step size of 0.05° 2θ and a count time of 1 s per step. Qualitative energy dispersive spectroscopy of LaTa-1200 was conducted using a using a Cameca SX-100 electron microprobe. LaTa-1200 is representative of the other two lanthanum tantalate phases as LaTa–OH is used as a starting material for both $LaTaO_4$ polymorphs. The microprobe analysis also provides information on sample homogeneity.

High-temperature XRD analyses of $Nd_2Ta_2O_7(OH)_2$ and $Pr_2Ta_2O_7(OH)_2$ were performed using a Scintag PAD X system equipped with a Buehler HDK 1.6 hot-stage. The diffractometer employed a sealed tube X-ray source (Cu $K\alpha$) and a peltier-cooled solid-state Ge detector. Diffraction patterns were collected in steps of 50 °C from room temperature up to 1200 °C. Scans parameters were 10–50° 2θ, 0.04° step-size, and 1 s count-time. Each scan required ~16 min. All runs were done in air atmosphere. The powder was placed on top of an alumina substrate, which was placed on the Pt/Rh heating strip. The surface temperature was calibrated based on the thermal expansion values of alumina, accurate to ±5 °C.

2.2. High-temperature drop solution calorimetry

Oxide melt drop-solution calorimetry in which a 5–8 mg pellet of sample is dropped into 20 g of sodium molybdate ($3Na_2O\cdot 4MoO_3$) solvent at 974 K was performed using a custom built Calvet microcalorimeter, following procedures described previously [32,33]. To aid dissolution, air was bubbled through the solvent. In addition, the sample was ground to a uniform micron-sized powder and the pellet was not pressed too tightly. Rapid and complete dissolution was verified by lack of baseline shifts during the calorimetric experiments, consistent measured enthalpies, and visual inspection of the solidified melt. The calorimeter was calibrated using ~5 mg pellets of α-Al_2O_3 (Alfa Aesar, 99.997 wt% metal basis). The measured enthalpies of drop solution (ΔH_{dsol}) were used to calculate the enthalpies of formation for the lanthanum tantalate samples.

3. Results and discussion

All the observed X-ray diffraction peaks matched those of previously reported [30,31] indicating pure phase. The microprobe analysis indicated that the sample was homogeneous. Only La, Ta, and O, were present, indicating that there were no additional contaminant elements, particularly potassium from the $K_7Na[Ta_6O_{19}]\cdot 14H_2O$ starting material. Previous characterization of LaTa–OH by Nyman et al. [30] also discounted the presence of citrate and additional water by TGA and IR analysis. To see a significant effect on calorimetric data, impurities must be present at a level of a few tenths of a percent or more and we are confident that no contaminants are found at these concentrations in the lanthanum tantalate samples.

The average ΔH_{dsol} (in kJ/mol) and two standard deviations of the mean were calculated from eight measurements and are summarized in Table 1. Previous high-temperature drop solution calorimetry experiments reported by McHale et al. [34] indicated that Ta_2O_5 does not dissolve rapidly enough in sodium molybdate solvent for accurate calorimetry, but metallic Ta oxidizes and dissolves. Using the following thermochemical cycle the enthalpy of drop solution for Ta_2O_5 can be calculated:

Ta (xl, 298 K)+5/4 O_2 (g, 974 K)→0.5 Ta_2O_5 (sln, 974 K)	ΔH_1 [34]
Ta_2O_5 (xl, 298 K)→2 Ta (xl, 298 K)+5/2 O_2 (g, 298 K)	ΔH_2 [35]
O_2 (g, 298 K)→ O_2 (g, 974 K)	ΔH_3 [36]
Ta_2O_5 (xl, 298 K)→Ta_2O_5 (sln, 974 K)	ΔH_4

$\Delta H_4 = 2\ \Delta H_1 + \Delta H_2 + 5/2\ \Delta H_3$

The measured enthalpy of drop solution for Ta metal ΔH_1 was provided by McHale et al. [34] as -991.6 ± 5.0 kJ/mol. The ΔH_2 value for Ta_2O_5 was reported by Panova et al. [35] as 2041.9 ± 6.3 kJ/mol. The ΔH_3 value, calculated by integrating the heat capacity from 298 to 974 K for O_2, is 22.7 kJ/mol [36]. The resulting value for the enthalpy of drop solution for Ta_2O_5 was calculated as 115.4 ± 8.0 kJ/mol.

Table 1
Enthalpy of drop solution ΔH_{drpsol} (kJ/mol) for LaTa–OH, LaTa-850, and LaTa-1200 in sodium molybdate solvent at 974 K. The average value and associated error (two standard deviations from the mean) is calculated from eight values.

$LaTaO_{3.5}(OH)$ (LaTa–OH)		$LaTaO_4$ (LaTa-850)		$LaTaO_4$ (LaTa-1200)	
(mg)	(kJ/mol)	(mg)	(kJ/mol)	(mg)	(kJ/mol)
5.84	63.519	6.94	42.889	8.65	36.409
4.96	62.048	5.65	39.392	6.89	39.433
5.20	71.241	6.20	41.864	8.13	41.325
5.25	73.442	6.30	37.299	7.98	39.216
4.86	75.817	7.36	39.135	8.20	37.413
5.24	64.034	5.67	40.987	8.74	37.880
5.67	60.548	6.20	35.910	7.31	35.322
5.73	63.288	5.25	42.976	6.10	38.733
	66.74 ± 4.12		40.06 ± 1.83		38.22 ± 1.33

Enthalpies of formation from the oxides ($\Delta H_{f\text{-}ox}$) and elements ($\Delta H_{f\text{-}el}$) for the lanthanum tantalate phases were calculated using the thermochemical cycles listed in Tables 2 and 3. To compare the lanthanum tantalate samples on a per mole basis, the calculated enthalpies of formation from the oxides and elements for LaTa–OH are based on one mole of La and Ta ($LaTaO_{3.5}(OH)$). These values indicate stable phases with respect to the binary oxides. The calculated $\Delta H_{f\text{-}el}$ indicates large stability with respect to La and Ta metal and H_2 and O_2 gas.

The $\Delta H_{f\text{-}ox}$ of $LnTaO_4$ (Ln=Sm, Eu, Gd, Ho, Er, Yb) were reported by Teterin et al., [37] and are shown in Table 4. These values were calculated from orbital interactions and range from −76 to −102 kJ/mol. The $\Delta H_{f\text{-}ox}$ values for the two $LaTaO_4$ polymorphs fall within this range and are situated between the values for $GdTaO_4$ (−81 kJ/mol) and $HoTaO_4$ (−98 kJ/mol). There is no obvious enthalpy trend as a function of ionic potential (Z/r) of the lanthanide cations for the rare-earth tantalate phases. Structural differences between the fergusonite structure adopted by $LnTaO_4$ (Ln=Sm, Eu, Gd, Ho, Er, Yb) and the orthorhombic structures that occur in the $LaTaO_4$ polymorphs may explain the absence of any trends related to the ionic potential of the lanthanide cations. Furthermore, the accuracy of the calculated values [37] is difficult to judge.

A study by Panova et al. [35] provides the calculated enthalpy of formation from the elements for $LnTaO_4$ based on their experimental values of enthalpies of formation for Ta_2O_5 and literature values for the lanthanum oxides. The $\Delta H_{f\text{-}el}$ for $LnTaO_4$ (Ln=Sm, Eu, Gd, Dy, Ho, Er, Yb) are listed in Table 4 and ranged from −3989.4 to −4066.3 kJ/mol, with a general trend of more exothermic values down the lanthanide series. The $\Delta H_{f\text{-}el}$ for the lanthanum tantalate samples based the enthalpies of drop solution obtained in this study are -2147.2 ± 9.5, -2012.1 ± 8.8, and -2010.3 ± 8.7 kJ/mol for LaTa–OH, LaTa-850, and LaTa-1200, respectively. The $\Delta H_{f\text{-}el}$ reported by Panova et al. [35] are more exothermic than the measured values, however, lack of details pertaining to the calculated $\Delta H_{f\text{-}el}$ values precludes additional analysis of the data.

The enthalpies of dehydration of LaTa–OH to LaTa-850 and the transformation of the LaTa-850 polymorph to the high temperature LaTa-1200 polymorph were calculated using the heats of drop solution. Thermochemical cycles used to calculate the enthalpies of transition (ΔH_{tr}) are summarized in Table 5. Dehydration of LaTa–OH to LaTa-850 at 25 °C is exothermic with a ΔH_{tr} of -15.64 ± 4.50 kJ/mol. The exothermic value for this reaction suggests that LaTa–OH is a metastable phase relative to LaTa-850 and is not a stable low-temperature hydrated form.

The transformation enthalpy of the lower temperature LaTa-850 phase to the higher temperature compound LaTa-1200 is slightly endothermic with a value of 1.84 ± 1.87 kJ/mol. Although the experimental errors put this value close to zero, it is likely that LaTa-850 is indeed thermodynamically stable at low temperature and the transition is likely to be thermodynamically reversible. The $T\Delta S$ term is generally small for solid-state reactions, thus the ΔG term usually follows similar trends to the ΔH. Previous

Table 4
The calculated heat of formation from the binary oxides ($\Delta H_{f\text{-}ox}$) [37] and elements ($\Delta H_{f\text{-}el}$) [35] for $LnTaO_4$ (Ln=Sm, Eu, Gd, Dy, Ho, Er, and Yb) compounds. The values for the La phases are the experimental values from the current study.

Compound	$\Delta H_{f\text{-}ox}$ (kJ/mol)	$\Delta H_{f\text{-}el}$ (kJ/mol)
$LaTaO_{3.5}(OH)$ (LaTa–OH)	-87.1 ± 9.6	-2147.2 ± 9.5
$LaTaO_4$ (LaTa-850)	-94.9 ± 8.8	-2012.1 ± 8.8
$LaTaO_4$ (LaTa-1200)	-93.1 ± 8.7	-2010.3 ± 8.7
$SmTaO_4$	−76	−3989.4
$EuTaO_4$	−76	−3843.1
$GdTaO_4$	−81	−3991.1
$DyTaO_4$		−4091.4
$HoTaO_4$	−98	−4114.0
$ErTaO_4$	−106	−4134.4
$YbTaO_4$		−4066.3

Table 2
Thermochemical cycles for calculation of $\Delta H_{f\text{-}ox}$ and $\Delta H_{f\text{-}el}$ for $LaTaO_{3.5}(OH)$ (LaTa–OH).

$LaTaO_{3.5}(OH)$ (xl, 298 K)→0.5 La_2O_3 (sln, 974 K)+0.5 Ta_2O_5 (sln, 974 K)+0.5 H_2O (g, 974 K)	$\Delta H_5=\Delta H_{drpsol}$
La_2O_3 (xl, 298 K)→La_2O_3 (sln, 974 K)	$\Delta H_6=-225.1 \pm 3.2$ kJ/mol [40]
Ta_2O_5 (xl, 298 K)→Ta_2O_5 (sln, 974 K)	$\Delta H_4=115.4 \pm 8.0$ kJ/mol [34]
H_2O (l, 298 K)→H_2O (g, 974 K)	$\Delta H_7=69.0$ kJ/mol [36]
0.5 La_2O_3 (xl, 298 K)+0.5 Ta_2O_5 (xl, 298 K)+0.5 H_2O (l, 298 K)→$LaTaO_{3.5}(OH)$ (xl, 298 K)	$\Delta H_8=\Delta H_{f\text{-}ox}$
$\Delta H_8=\Delta H_{f\text{-}ox}=-\Delta H_5+0.5\ \Delta H_6+0.5\Delta H_4+0.5\ \Delta H_7=$ **-87.1 ± 9.6 kJ/mol**	
2 La(xl, 298 K)+1.5 O_2(g, 298 K)→La_2O_3 (xl, 298 K)	$\Delta H_9=-1792.46 \pm 2.67$ [41]
2 Ta(xl, 298 K)+2.5 O_2 (g, 298 K)→Ta_2O_5 (xl, 298 K)	$\Delta H_2=-2041.9 \pm 6.3$ [35]
H_2 (g, 298 K)+0.5 O_2 (g, 298 K)→H_2O (l, 298 K)	$\Delta H_{10}=-285.8 \pm 0.1$ [36]
La (xl, 298 K)+Ta (xl, 298 K) +0.5 H_2 (g, 298 K)+2.25 O_2(g, 298 K)→$LaTaO_{3.5}(OH)$ (xl, 298 K)	$\Delta H_{11}=\Delta H_{f\text{-}el}$
$\Delta H_{11}=\Delta H_{f\text{-}el}=\Delta H_8+0.5\ \Delta H_9+0.5\ \Delta H_2+0.5\Delta H_{10}=$ **-2147.2 ± 9.5 kJ/mol**	

Table 3
Thermochemical cycles for calculation of $\Delta H_{f\text{-}ox}$ and $\Delta H_{f\text{-}el}$ for the $LaTaO_4$ polymorphs (LaTa-850 and LaTa-1200).

$LaTaO_4$ (xl, 298 K)→La_2O_3 (sln, 974 K)+Ta_2O_5 (sln, 974 K)		$\Delta H_{12}=\Delta H_{drpsol}$
La_2O_3 (xl, 298 K)→La_2O_3 (sln, 974 K)		$\Delta H_6=-225.1 \pm 3.2$ kJ/mol [40]
Ta_2O_5 (xl, 298 K)→Ta_2O_5 (sln, 974 K)		$\Delta H_4=115.4 \pm 8.0$ kJ/mol
0.5 La_2O_3 (xl, 298 K)+0.5 Ta_2O_5 (xl, 298 K)→$LaTaO_4$ (xl, 298 K)		$\Delta H_{13}=\Delta H_{f\text{-}ox}$
$\Delta H_{13}=\Delta H_f=-\Delta H_{12}+0.5\ \Delta H_6+0.5\ \Delta H_4$		
LaTa-850	$\Delta H_{f\text{-}ox}=$ **-94.9 ± 8.8 kJ/mol**	
$LaTaO_4$-1200	$\Delta H_{f\text{-}ox}=$ **-93.1 ± 8.7 kJ/mol**	
2 La(xl, 298 K)+0.75 O_2(g, 298 K)→La_2O_3 (xl, 298 K)		$\Delta H_9=-1792.46 \pm 2.67$ [41]
2 Ta(xl, 298 K)+2.5 O_2 (g, 298 K)→Ta_2O_5 (xl, 298 K)		$\Delta H_2=-2041.9 \pm 6.3$ [35]
La(xl, 298 K)+Ta (xl, 298 K)+2 O_2(g, 298 K)→$LaTaO_4$ (xl, 298 K)		$\Delta H_{14}=\Delta H_{f\text{-}el}$
$\Delta H_{14}=\Delta H_{13}+\ 0.5\ \Delta H_9+0.5\ \Delta H_2$		
LaTa-850	$\Delta H_{f\text{-}el}=$ **-2012.1 ± 8.8 kJ/mol**	
$LaTaO_4$-1200	$\Delta H_{f\text{-}el}=$ **-2010.3 ± 8.7 kJ/mol**	

high-temperature XRD analysis of the lanthanum tantalate samples reported by Nyman et al. [31] indicate that transition from the lower temperature $LaTaO_4$ to the higher temperature phase occurs at approximately 1050 °C. This implies entropy of transition $=\Delta H_{tr}/T_{tr}=1840/1323=1.8$ J/mol K, which is reasonable for a solid–solid transition.

Given that LaTa-850 appears to be the energetically most stable phase among the lanthanum tantalate samples, one can then turn to the crystal structure to gain insight into possible reasons for its stability. All three compounds possess a similar structure with alternating lanthanum and tantalate sheets linked into a framework topology (Fig. 1) [31]. The major structural differences between the lanthanum tantalate samples are the corrugation of the tantalate layer in both LaTa–OH and LaTa-1200. The corrugation of the layers originates from the bridging of the TaO_6 octahedra. The bridging of the Ta atoms in LaTa–OH occurs through four equatorial and one axial oxygen atoms, effectively creating Ta_2O_{10} dimers that are linked through vertex-sharing into a two-dimensional corrugated sheet. The corrugation of the tantalate layer for LaTa-1200 stems from bridging two axial and three equatorial oxygen atoms between the tantalum atoms. All of the bonding between the tantalate octahedra in LaTa-850 occurs through vertex-sharing of the equatorial oxygen atoms, resulting in a flattened tantalate sheet.

When contemplating trends in compound stability, one can qualitatively assess the effect of the lattice energies on the overall energetics of the system [38]. The lattice energy is the molar energy change accompanying the formation of a solid from its separated ionic components. The largest contributions to the lattice energy are the electrostatic interactions (75–90%), with additional contribution from repulsive components (10–20%) [38]. The size and charge of the cations in the structure affect the lattice energies and interatomic distance between two higher valence ions, which in turn can affect the electrostatic and repulsive components.

There are no systematic or major differences in the metal to oxygen bonds that could explain the changes in stability observed for these compounds [30,31]. Thus, the energetics of the lanthanum tantalate compounds are likely to be influenced by small differences in interatomic distances of the high valency Ta^{5+} and La^{3+} cations and the resulting cation repulsion. The interatomic distances between the Ta^{5+} and La^{3+} cations are summarized in Table 6.

First consider the interatomic distances between the lanthanum cations. The La^{3+}–La^{3+} interatomic distances are 4.137 and 4.168 Å for edge-sharing between the La polyhedra in LaTa–OH and LaTa-1200. In both compounds, the distance decreases slightly (3.93 Å) when the La polyhedra share a face. A range of

Table 5
Thermochemical cycles used to calculate the enthalpies of transition (ΔH_{tr}) for the lanthanum tantalate samples.

$LaTaO_{3.5}$(OH) (xl, 298 K)→0.5 La_2O_3 (sln, 974 K)+0.5 $Ta2O_5$ (sln, 974 K)+0.5 H_2O (g, 974 K)	ΔH_5
$LaTaO_4$ (xl, 298 K)→0.5 La_2O_3 (sln, 974 K)+0.5 Ta_2O_5 (sln, 974 K)	ΔH_{12}(LaTa-850)
H_2O (l, 298 K)→H_2O (g, 974 K)	ΔH_7 [36]
$La_2Ta_2O_7(OH)_2$ (xl, 298 K)→2 $LaTaO_4$ (LaTa-850) (xl, 298 K)+H_2O (l, 298 K)	$\Delta H_{15}=\Delta H_{tr}$
$\Delta H_{15}=-2\ \Delta H_{12}-\Delta H_7+2\ \Delta H_5$	
$\boldsymbol{\Delta H_{15}=\Delta H_{tr}=-15.64\pm4.50}$ **kJ/mol**	
$LaTaO_4$ (xl, 298 K)→$LaO_{1.5}$ (sln, 974 K)+$TaO_{2.5}$ (sln, 974 K)	ΔH_{12}(LaTa-850)
$LaTaO_4$ (xl, 298 K)→$LaO_{1.5}$ (sln, 974 K)+$TaO_{2.5}$ (sln, 974 K)	ΔH_{12}(LaTa-1200)
$LaTaO_4$(LaTa-850) (xl, 298 K)→$LaTaO_4$ (LaTa-1200) (xl, 298 K)	$\Delta H_{16}=\Delta H_{tr}$
$\Delta H_{16}=-\Delta H_{12}$(LaTa-1200)+$\Delta H_{12}$(LaTa-850)	
$\boldsymbol{\Delta H_{16}=\Delta H_{tr}=1.84\pm1.87}$ **kJ/mol**	

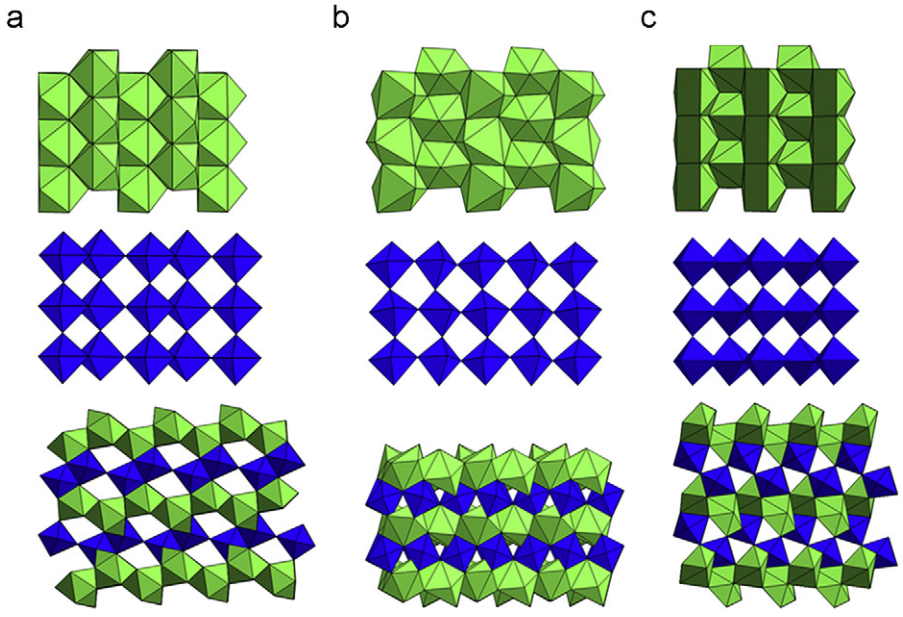

Fig. 1. The polyhedral representations of (a) LaTa–OH, (b) LaTa-850, and (c) LaTa-1200 [30,31]. The sheets of La polyhedra (green) are shown on the top, sheets of Ta octahedral (blue) are in the middle and the stacking between the sheets are illustrated on the bottom. (For interpretation of the references to color in this figure legend, the reader is referred to the web version of this article.)

Table 6
The average and range of bond distances for the rare-earth tantalate samples [30,31,42,43].

Sample	*Ln*–*Ln* distances (Å)—edge	*Ln*–*Ln* distances (Å)—face	Ta–Ta distances (Å)—vertex	Ta–Ta distances (Å)—edge	*Ln*–Ta distances (Å)—vertex	*Ln*–Ta distances (Å)—face	*Ln*–Ta distances (Å)—edge
$LaTaO_{3.5}(OH)$ [30]	4.130, 4.137	3.930	3.930	3.243	4.195	3.428, 3.432	
LaTa-850 [31]	3.916, 4.186, 4.229, 4.402		3.736, 3.918		3.540–3.768		
LaTa-1200 [31]	4.168	3.931	3.780, 3.981		3.815, 4.264	3.487, 3.625	
$PrTaO_{3.5}(OH)$	4.017, 4.093	3.904	3.904	3.241	4.047	3.391, 3.443	
$NdTaO_{3.5}(OH)$	4.081, 4.086	3.894	3.814	3.192	4.209	3.339, 3.376	
$NdTaO_4$-850 [42]	3.776, 4.019			3.424	3.966, 4.012, 4.055, 4.057		3.569, 3.618, 3.667
$NdTaO_4$-1200 [43]	3.821, 3.918			3.380	3.959, 3.960		3.587, 3.783

distances is observed for LaTa-850 (3.916–4.402 Å) even with the absence of face-sharing polyhedra. The wide range of observed interatomic distances for different bonding modes indicates that the La^{3+}–La^{3+} interatomic distances are flexible and may not have a large impact on the energetics of the system.

When one considers the differences in the Ta^{5+}–Ta^{5+} interatomic distances, relationships between the distances and the bonding modes can be observed. There are two distinct interatomic Ta^{5+}–Ta^{5+} distances: 3.736–3.981 Å corresponding to vertex sharing between the Ta^{5+} polyhedra and 3.243 Å resulting from the formation of the Ta_2O_{10} dimers. Decreasing the interatomic distance between high valence cations, particularly Ta^{5+}, should increase the repulsive component of the lattice energy and decrease the overall stability of the structure. The shared edges of the Ta^{5+} dimer in LaTa–OH significantly decrease the distance between the Ta atoms and could result in a less stable structure compared to the $LaTaO_4$ polymorphs. The experimental enthalpies of formation are less exothermic than these of the $LaTaO_4$ phases and the exothermic enthalpy of reaction to the higher temperature phases indicate that the hydrated phase is indeed metastable.

Face-sharing between the La and the Ta polyhedra also decrease the La^{3+}–Ta^{5+} interatomic distance, but the destabilizing affect may be lessened due to the lower charge on the La^{3+} cation. There is little difference in the Ta^{5+}–Ta^{5+} or the La^{3+}–Ta^{5+} distances for the $LaTaO_4$ polymorphs and this may account for the similarities in the measured enthalpies of formation. However, the lack of shared Ta^{5+}–Ta^{5+} or La^{3+}–Ta^{5+} polyhedral faces in LaTa-850 may have a slight stabilizing effect, resulting in the most energetically stable phase.

To investigate the effects of the cation–cation repulsion on the stability of the rare-earth tantalates, additional experiments with smaller lanthanide cations (Pr^{3+}, Nd^{3+}) were attempted. Following the lanthanide contraction, the ionic radii of the eight-coordinated La, Pr, and Nd cations are 1.16, 1.12 and 1.11 Å, respectively [39]. The Ln^{3+}–Ta^{5+}, Ta^{5+}–Ta^{5+}, and Ln^{3+}–Ln^{3+} (*Ln*=Pr, Nd) distances for the PrTa–OH and NdTa–OH analogues are summarized in Table 6. With smaller lanthanide radii, the unit cell volume decreases: 374.22 $Å^3$ (La), 364.63 $Å^3$ (Pr), and 361.49 $Å^3$ (Nd). Comparing the La and Nd analogues, all cation–cation distances decrease, except for the vertex-shared Ln^{3+}–Ta^{5+} distance which increases slightly. The distances that decrease the most are the Ta^{5+}–Ta^{5+} vertex-sharing and the Ln^{3+}–Ta^{5+} face-sharing, both decreasing by around 0.1 Å, and the Pr analogue follows this trend as well. The Pr-analogue does not follow these trends for every metal–metal distance; it exhibits the smallest *Ln*–*Ln* edge and *Ln*–Ta vertex distances of the three polymorphs. Perhaps it is this decrease in the Ta^{5+}–Ta^{5+} distance as the Ln^{3+} ion decreases that eventually destabilizes the *Ln*Ta–OH lattice, in that it cannot be formed pure beyond *Ln*=Nd.

As with the LaTa–OH compound [31], we carried out high-temperature X-ray diffraction on the Pr and Nd analogues to follow the thermal decomposition and formation of the respective orthotantalates. They both undergo the same weight loss associated with dehydration at 600 °C and crystallize around 800 °C. However, the phase changes are not clean, multiple $LnTaO_4$ polymorphs co-exist for both, and well-crystallized samples are not observed until much higher temperatures. With the Nd-analogue, monoclinic *P*2/*c* (#13) $NdTaO_4$ [42] is first observed around 850 °C, and the analogue to LaTa-850 is not seen at all. For the Pr-analogue, we observe only the *P*2/*c* polymorph at 800 °C. The analogue to LaTa-850 co-exists with the *P*2/*c* polymorph at 875 °C, but is never formed pure. At 1200 °C, for both the Nd and Pr analogues, the main $LnTaO_4$ polymorph is monoclinic *I*2/*a* (#15).

The cation–cation distances for the two $NdTaO_4$ polymorphs are summarized in Table 6 for comparison to the other rare-earth tantalate phases. Although we observe the Pr-analogues of these two monoclinic phases, they have not been reported; perhaps an indication of the inability to form these as pure phases. We note the similarities between these polymorphs: both in the types of polyhedra-connectivity as well as the observed cation–cation distances, which in accordance with previous discussion suggest very similar stabilities. Perhaps this is why we cannot obtain these phases cleanly or pure unless very high annealing temperatures are applied.

The La^{3+} cation is the largest of the rare-earth cations and may benefit the most from minimizing the cation–cation repulsion. The ability to isolate an intermediate phase (LaTa-850) that seems unique to the rare-earths suggests that this phase is indeed the energetically favored phase and that cation–cation repulsion may be lessened. The presence of several coexisting polymorphs for the Pr tantalate system suggests that there is essentially no stability field for the Pr intermediate, per the above discussion. The other factor that may come into play is the conformation of the layers. All the rare-earth tantalate phases discussed above are composed of corrugated layers of Ta polyhedra alternating with corrugated layers of *Ln* polyhedra, with the exception of LaTa-850. The relatively flat layers of LaTa-850 may limit the size range for the *Ln*-polyhedra, since there is less flexibility for distortion within flat layers than within corrugated layers.

This work suggests that the La-850 polymorph may only be found for the lanthanum tantalate system. Variable temperature powder X-ray diffraction experiments with praseodymium tantalate imply other phases could be synthesized, however purification of these phases may be difficult. These results indicate that

additional synthesis and characterization of the rare-earth tantalates are necessary to isolate novel phases.

These results directly affect interest in Eu-substituted rare-earth tantalate phases as phosphors. The orthotantalate polymorph, for instance, is sensitive to the rare-earth radius, which varies with the dopant concentration. Our preliminary studies show that the polymorph of $LaTaO_4$:Eu changes with Eu concentration, rendering an intriguingly complex system for fine-tuning of luminescent properties. These current studies have aided in clarifying structural parameters that ultimately control phase formation, transition and stability.

4. Conclusions

The enthalpies of formation for three lanthanum tantalate samples (LaTa–OH, LaTa-850 and LaTa-1200) were measured using the high-temperature oxide melt solution calorimetry. The enthalpies of formation indicate that all phases are stable with respect to the binary oxides and the elements. Enthalpies of reaction between the phases indicate that the low temperature hydrated phase (LaTa–OH) is metastable with respect to the $LaTaO_4$ polymorphs (LaTa-850 and LaTa-1200). The relative instability of this phase may be explained by the presence of shared TaO_6 edges that result in smaller interatomic distances between the Ta^{5+} cations. There are little differences in the enthalpies of formation for the two $LaTaO_4$ polymorphs, but LaTa-850 is likely the most energetically stable phase. The stability of LaTa-850 may be related to small changes in the structure that result in longer interatomic distances between the lanthanum and tantalum cations. Additional studies on Pr^{3+} and Nd^{3+} tantalates also suggest that cation–cation repulsions may play a role in the stability of the LaTa-850.

Acknowledgments

The work at U.C. Davis was supported by DOE Grant DE-FG02-03ER46053. We thank Dr. Sarah Roeske and Brian Joy (U.C. Davis) for their assistance on the electron microprobe. Work at Sandia National Laboratories was supported by Sandia's Solid-State-Lighting Science Energy Frontier Research Center, funded by the U.S. Department of Energy, Office of Science, Office of Basic Energy Sciences.

Sandia National Laboratories is a multi-program laboratory operated by Sandia Corporation, a wholly owned subsidiary of Lockheed Martin company, for the U.S. Department of Energy's National Nuclear Security Administration under Contract DE-AC04-94AL85000.

Appendix A. Supplementary material

Supplementary data associated with this article can be found in the online version at doi:10.1016/j.jssc.2010.08.024.

References

[1] T.G.N. Babu, J. Koshy, J. Solid State Chem. 126 (1996) 202–207.
[2] V. Thangadurai, W. Weppner, Adv. Funct. Mater. 15 (2005) 107–112.
[3] F.E. Osterloh, Chem. Mater. 20 (2008) 35–54.
[4] S. Arakawa, T. Shiotsu, S. Hayashi, J. Ceram. Soc. Jpn. 113 (2005) 317–319.
[5] R. Haugsrud, T. Norby, Nat. Mater. 5 (2006) 193–196.
[6] T. Minamidani, G. Shinomiya, S. Chikutei, T. Kondo, T. Sakata, H. Mori, N. Imanaka, G. Adachi, Nip. Kag. Kaishi. (1993) 656–664.
[7] I. Arellano, M. Nazarov, C.C. Byeon, E.J. Popovici, H. Kim, H.C. Kang, D.Y. Noh, Mater. Chem. Phys. 119 (2010) 48–51.
[8] A. Hristea, E.J. Popovici, L. Muresan, M. Stefan, R. Grecu, A. Johansson, M. Boman, J. Alloys Compd. 471 (2009) 524–529.
[9] B. Liu, K. Han, X.L. Liu, M. Gu, S.M. Huang, C. Ni, Z.M. Qi, G.B. Zhang, Solid State Commun. 144 (2007) 484–487.
[10] W.P. Liu, Q.L. Zhang, L.H. Ding, D.L. Sun, J.Q. Luo, S.T. Yin, J. Alloys Compd. 474 (2009) 226–228.
[11] E.J. Popovici, F. Imre-Lucaci, L. Muresan, M. Stefan, E. Bica, R. Grecu, E. Indrea, J Optoelectron. Adv. Mater. 10 (2008) 2334–2337.
[12] X.Z. Xiao, B. Yan, J. Mater. Res. 23 (2008) 679–687.
[13] X. Tang, H. Ye, Z. Zhao, H. Liu, C. Ma, Catal. Lett. 133 (2009) 362–369.
[14] S.C. Yan, Z.Q. Wang, Z.S. Li, Z.G. Zou, Solid State Ionics 180 (2009) 1539–1542.
[15] M. Tian, W. Shangguan, J. Yuan, L. Jiang, M. Chen, J. Shi, Z. Ouyang, S. Wang, Appl. Catal. A: Gen 309 (2006) 76–84.
[16] K. Shimizu, S. Itoh, T. Hatamachi, T. Kodama, M. Sato, K. Toda, Chem. Mater. 17 (2005) 5161–5166.
[17] M. Machida, K. Miyazaki, S. Matsushima, M. Arai, J. Mater. Chem. 13 (2003) 1433–1437.
[18] M. Machida, J.-i. Yabunaka, T. Kijima, Chem. Mater. 12 (2000) 812–817.
[19] S. Zhang, G. Zhang, S. Yu, X. Chen, X. Zhang, J. Phys. Chem. C 113 (2009) 20029–20035.
[20] L.M. Torres-Martinex, L.L. Garza-Tovar, M.E. Meza-de la Rosa, A. Maartinez-de la Cruz, A. Cruz-Lopez, Mater. Sci. Forum. 554–555 (2007) 103–106.
[21] R. Haugsrud, T. Norby, J. Am. Ceram. Soc. 90 (2007) 1116–1121.
[22] M. Nyman, M.A. Rodriguez, L.E. Shea-Rohwer, J.E. Martin, P.P. Provencio, J. Am. Chem. Soc. 131 (2009) 11652–11655.
[23] R.B. Ferguson, Can. Mineral 6 (1957) 72–77.
[24] A.I. Komkov, Dok. Akad. Nauk. SSR 136 (1959) 753–754.
[25] V.S. Stubican, J. Am. Ceram. Soc. 47 (1964) 55–58.
[26] M.S. Slobodyanik, A.O. Kapshuk, N.M. Belyavina, V.Y. Markiv, A.M. Sich, Y.O. Titov, Dop. Nat. Akad. Nauk Ukraini. (2003) 140–145.
[27] A. Belous, O. Gavrilenko, O. Pashkova, C. Galven, O. Bohnke, Eur. J. Inorg. Chem. 8 (2006) 1552–1560.
[28] K. Toda, T. Honma, Z.G. Ye, M. Sato, J. Alloys Compd 249 (1997) 256–259.
[29] K. Toda, K. Uematsu, M. Sato, J. Ceram. Soc. Jpn. 105 (1997) 482–485.
[30] M. Nyman, M.A. Rodriguez, T.M. Alam, T.M. Anderson, A. Ambrosini, Chem. Mater. 21 (2009) 2201–2208.
[31] M. Nyman, M.A. Rodriguez, L.E.S. Rohwer, J.E. Martin, M. Waller, F.E. Osterloh, Chem. Mater. 21 (2009) 4731–4737.
[32] A. Navrotsky, Phys. Chem. Mineral 24 (1997) 222–241.
[33] A. Navrotsky, Phys. Chem. Mineral 2 (1977) 89–104.
[34] J.M. McHale, A. Navrotsky, Chem. Mater. 9 (1997) 1538–1546.
[35] T.I. Panova, E.N. Isupova, E.K. Keler, Inorg. Mater. 14 (1978) 616–617.
[36] R.A. Robie, B.S. Hemingway, in: Thermodynamic Properties of Minerals and Related Substances at 298.15 K and 1 bar (104 Pascals) Pressure and at Higher Temperatures, U.S. Geological Bulletin, Washington, DC, 1995.
[37] G.A. Teterin, E.M. Menchuk, B.F. Zinchenko, L.P. Eremina, Ukrain. Khimich. Z. 62 (1996) 82–84.
[38] S. Stolen, T. Grande, N.L. Allan, in: Chemical Thermodynamics of Materials: Macroscopic and Microscopic Aspects, John Wiley & Sons Ltd., West Sussex, England, 2004.
[39] R.D. Shannon, Acta Crystal. A 32 (1976) 751–757.
[40] J.H. Cheng, A. Navrotsky, X.D. Zhou, H.U. Anderson, J. Mater. Res. 20 (2005) 191–200.
[41] E.H.P. Cordfunke, R.J.M. Konings, Thermochim. Acta 375 (2001) 65–79.
[42] M. Kapon, G.M. Reisner, Kristallograf. 46 (1990) 349–350.
[43] A. Santoro, M. Marezio, R.S. Roth, D. Minor, J. Solid State Chem. 35 (1980) 167–175.